

## Stresses near the edge of bonded dissimilar materials described by two stress intensity factors

D. MUNZ and Y.Y. YANG

University Karlsruhe and Nuclear Research Center Karlsruhe, Germany

Received 15 October 1991; accepted in revised form 26 May 1992

**Abstract.** Stresses near the free edges of the interface of bonded dissimilar materials can be described by the sum of a regular stress term and one or two stress singularity terms. A method for the calculation of the corresponding stress intensity factors from finite element results is presented which is useful to determine two stress intensity factors together. Results for some geometries show that all three terms may contribute significantly to the stress distribution near the free edge of the interface for thermal stress.

### 1. Introduction

In Fig. 1 the general configuration at the interface of bonded dissimilar materials is shown which is characterized by the angles  $\theta_1$  and  $\theta_2$ . The stresses near the free edge of the interface can be described by

$$\sigma_{ij}(r, \theta) = \sum_{k=0}^N \frac{K_k}{(r/L)^{\omega_k}} f_{ijk}(\theta), \quad (1)$$

where  $r$  and  $\theta$  are defined in Fig. 1 and  $L$  is a characteristic length of the component. The angular functions  $f_{ijk}$  and the stress intensity factors  $K_k$  are defined in such a way, that  $f_{\theta k}(\theta = 0) = 1$  ( $k = 0, 1, \dots, N$ ).  $\omega_k$  and  $f_{ijk}$  depend on the elastic constants  $E_1, \nu_1, E_2, \nu_2$  and on the angles  $\theta_1$  and  $\theta_2$ , but are independent of the loading conditions. They can be calculated analytically by solving the general stress function taking into account the boundary conditions

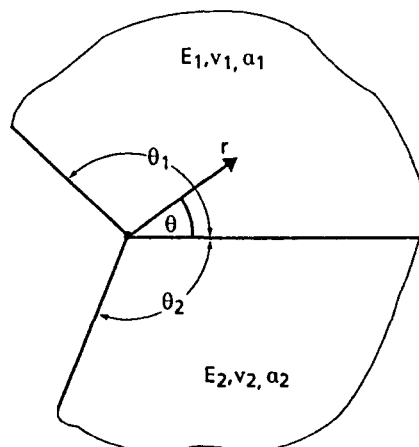


Fig. 1. General configuration at the free edge of a joint.

at  $\theta = 0$ ,  $\theta_1$  and  $\theta_2$  [1]. The resulting  $\omega_k$  can be positive real, negative real or complex. For complex values of  $\omega_k$  (1) is no longer useful and separate considerations are necessary [1, 2]. For  $\omega_k > 0$  a stress singularity exists. One solution for  $\omega_k$  is  $\omega_0 = 0$  leading to a stress term, which is independent of  $r$

$$\sigma_{ij0}(\theta) = K_0 f_{ij0}(\theta). \quad (2)$$

Instead of  $K_0$ , the designation  $\sigma_0$  is used in the following text. This term can be calculated analytically for any combination of angles  $\theta_1$ ,  $\theta_2$  and any loading condition [3].

The other stress intensity factors  $K_k$  ( $k = 1, 2, \dots, N$ ) have to be calculated numerically from the stress distribution for small values of  $r$ , for instance by using the finite element method. They depend on the material properties, the applied loading condition and the geometry of the component.

If, besides  $\omega_0 = 0$ , more than one value of  $|\omega_k|$  is less than about 0.5, then all of them may contribute to the stress field near the edge of the interface. This will be shown in this paper and the corresponding values of  $K_k$  are calculated for some examples.

## 2. Method of determination of several stress intensity factors

For two  $\omega_k > 0$  Knesl et al. [4] calculated the two stress intensity factors for mechanical loading. They first obtained  $K_1$  from the stress distribution for small  $r$  neglecting the second term and then  $K_2$  from the stress distribution at larger  $r$  taking into account the first term. Theocaris [5] used a similar method. In many cases this method cannot be applied, because the term with  $k = 2$  contributes significantly to the stress distribution also very close to the free edge of the interface as will be shown in the examples in Section 3. Therefore it is necessary to develop a method by which two or more stress intensity factors can be determined simultaneously. In the following such a method is presented.

Equation (1) can be rewritten by using (2) as

$$\sigma_{ij}(r, \theta) = \sum_{k=1}^N \frac{K_k}{(r/L)^{\omega_k}} \cdot f_{ijk}(\theta) + \sigma_{ij0}(\theta), \quad (3)$$

where  $\omega_k$ ,  $\sigma_{ij0}$  and  $f_{ijk}$  can be obtained analytically. By the finite element method the stresses  $\sigma_{ij}^{FE}(r, \theta)$  can be calculated. Then a quantity  $\Pi_{ij}$  is defined as

$$\Pi_{ij} = \sum_{l=1}^M \left\{ \sigma_{ij}^{FE}(r_l, \theta_l) - \sigma_{ij0}(\theta_l) - \sum_{k=1}^N \frac{K_k}{(r_l/L)^{\omega_k}} f_{ijk}(\theta_l) \right\}^2. \quad (4)$$

$M$  is the number of points used for determining  $K_k$ . According to the least squares method, the minimum of  $\Pi_{ij}$  with respect to the values of  $K_k$  has to be found. It is given by

$$\frac{\partial \Pi_{ij}}{\partial K_k} = 0 \quad (5)$$

leading to  $N$  equations

$$\sum_{k=1}^N K_k \sum_{l=1}^M \frac{1}{(r_l/L)^{\omega_k}} f_{ijk}(\theta_l) \cdot \frac{1}{(r_l/L)^{\omega_q}} f_{ijq}(\theta_l) = \sum_{l=1}^M [\sigma_{ij}^{FE}(r_l, \theta_l) - \sigma_{ij0}(\theta_l)] \frac{1}{(r_l/L)^{\omega_q}} f_{ijq}(\theta_l), \quad (6)$$

with  $q = 1, 2, \dots, N$ . The values of  $K_k$  are obtained by solving these equations.

### 3. Results

The method given in Section 2 can be used for any geometry, material combinations and loading conditions. To show the applicability of the method two geometries are chosen somewhat arbitrarily. With these examples the general behavior of joints can be discussed.

Cooling down of the joint by  $\Delta T$  is considered as one loading condition. The stresses are proportional to  $\Delta T$ . All results for  $\sigma_{ij}$  and  $K_k$  are given for  $\Delta T = -1^\circ\text{C}$ .

A second loading is mechanical loading with a constant load distribution applied at the upper and lower surfaces.

The selected geometries are shown in Fig. 2. For convenience symmetric joints are considered. The angles are  $\theta_1 = 165^\circ, \theta_2 = -55^\circ$  (combination A) and  $\theta_1 = 115^\circ, \theta_2 = -45^\circ$  (combination B).

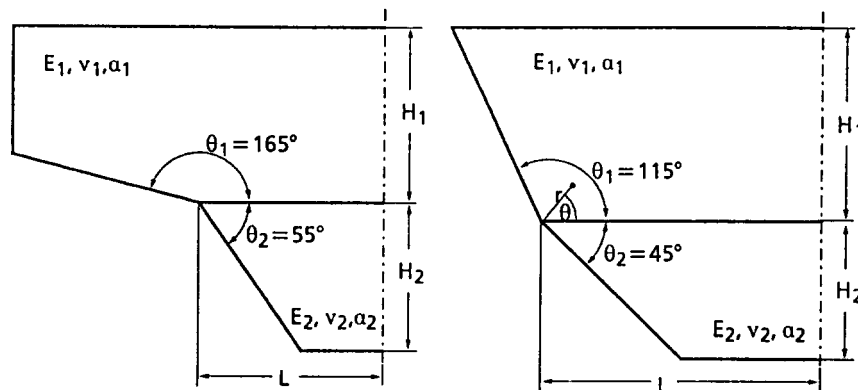
The stress exponents  $\omega_k$  have been calculated for the material parameters  $E_1 = 280 \text{ GPa}$ ,  $\nu_1 = 0.26, \nu_2 = 0.3$  and variable  $E_2$ . The values of  $\omega_k$  for which  $|\text{Re}(\omega)| < 0.5$  are plotted in Fig. 3 versus  $E_2/E_1$ . The complex exponents are described by  $\omega = s + ip$ .

Different ranges of  $E_2/E_1$  can be distinguished:

Combination A:

$E_2/E_1 < 0.0182 \quad \omega_1 < 0, \omega_2 < 0$  (no singularity term),

$0.0182 < E_2/E_1 < 8.51 \quad \omega_1 > 0, \omega_2 < 0$  (one singularity term),



A

B

Fig. 2. Geometries of investigated joints (A:  $L/H_1 = 1.016, L/H_2 = 1.233$ , B:  $L/H_1 = 1.424, L/H_2 = 1.986$ ).

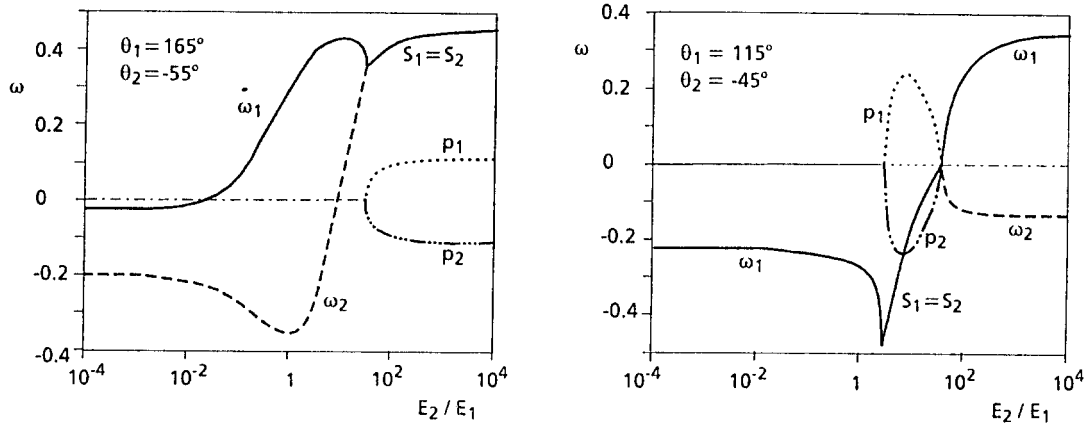


Fig. 3. Stress exponent  $\omega$  versus  $E_2/E_1$  ( $E_1 = 280$  GPa,  $\nu_1 = 0.26$ ,  $\nu_2 = 0.3$ ).

$8.51 < E_2/E_1 < 30.35$      $\omega_1 > 0, \omega_2 > 0$  (two singularity terms),  
 $E_2/E_1 > 30.35$          $\omega_1$  and  $\omega_2$  complex ( $s_1 = s_2 > 0, p_1 > 0, p_2 < 0$ ).

Combination B:

$E_2/E_1 < 3.931$          $\omega_1 < 0$ , no  $|\text{Re}(\omega_2)| < 0.5$  (no singularity term),  
 $3.931 < E_2/E_1 < 43.61$      $\omega_1$  and  $\omega_2$  complex,  $s_1 = s_2 < 0, p_1 > 0, p_2 < 0$ ,  
 $E_2/E_1 > 43.61$          $\omega_1 > 0, \omega_2 < 0$  (one singularity term).

The angular functions and the  $\sigma_{ij0}$  terms can be represented as

$$f_{jrk}(\theta) = \{A_{jk}(2 + \omega_k) \sin(\omega_k \theta) + B_{jk}(2 + \omega_k) \cos(\omega_k \theta) - C_{jk}(2 - \omega_k) \sin[(2 - \omega_k)\theta] - D_{jk}(2 - \omega_k) \cos[(2 - \omega_k)\theta]\} / \{(2 - \omega_k)(B_{jk} + D_{jk})\}, \quad (7a)$$

$$f_{j\theta k}(\theta) = \{A_{jk} \sin(\omega_k \theta) + B_{jk} \cos(\omega_k \theta) + C_{jk} \sin[(2 - \omega_k)\theta] + D_{jk} \cos[(2 - \omega_k)\theta]\} / (B_{jk} + D_{jk}), \quad (7b)$$

$$f_{jr\theta k}(\theta) = -\{A_{jk} \omega_k \cos(\omega_k \theta) - B_{jk} \omega_k \sin(\omega_k \theta) + C_{jk}(2 - \omega_k) \cos[(2 - \omega_k)\theta] - D_{jk}(2 - \omega_k) \sin[(2 - \omega_k)\theta]\} / \{(2 - \omega_k)(B_{jk} + D_{jk})\}, \quad (7c)$$

$$\sigma_{j\theta 0}(\theta) = 2(A_{j0}\theta + B_{j0} - C_{j0} \sin(2\theta) - D_{j0} \cos(2\theta)), \quad (8a)$$

$$\sigma_{j\theta 0}(\theta) = 2(A_{j0}\theta + B_{j0} + C_{j0} \sin(2\theta) + D_{j0} \cos(2\theta)), \quad (8b)$$

$$\tau_{jr\theta 0}(\theta) = -2(\frac{1}{2}A_{j0} + C_{j0} \cos(2\theta) - D_{j0} \sin(2\theta)), \quad (8c)$$

with  $j = 1, 2$  for the two materials.

In agreement with (2),  $\sigma_0 = 2(B_{j0} + D_{j0})$ .

It can be shown that the regular stress terms  $\sigma_{ij0}$  are proportionate to  $\alpha_1(1 + \nu_1) - \alpha_2(1 + \nu_2)$  for plane strain [6]. For the following calculations  $\alpha_1 = 2.5 \times 10^{-6}/\text{K}$  and  $\alpha_2 = 18.95 \times 10^{-6}/\text{K}$  have been chosen. The stresses in the joint have been calculated with the FE-code ABAQUS. The stress intensity factors have been determined from the FE-results of  $\sigma_\theta$

at  $\theta = 0$ . Different values of  $M$  in (6) according to different ranges of  $r/L$  have been used. The lower bound was fixed to  $(r/L)_{\min} = 1.6 \times 10^{-5}$ .

Results of  $K_k$  as a function of the selected upper bound  $(r/L)_{\max}$  for combination A with  $E_2/E_1 = 21.42$  and for combination B with  $E_2/E_1 = 50$  are shown in Fig. 4 for thermal loading. In both cases the values of  $K_k$  are calculated for two terms ( $N = 2$ ). There is a range where the determined  $K$ -values are nearly constant. If the upper limit of the selected range in  $r/L$  is too high, there will be deviations because terms with  $N > 2$  are important. If the upper limit is too low there will be deviations, because of inaccuracies in the FE-results [7]. The range of  $1.6 \times 10^{-5} < r/L < 5 \times 10^{-4}$  was used to determine the stress intensity factors.

In Fig. 5 the parameters  $\omega_1, \omega_2, K_1, K_2$  and  $\sigma_0$  are plotted versus  $E_2/E_1$  for combination A in the range where  $\omega_1$  and  $\omega_2$  are real. It can be seen that  $\sigma_0$  approaches infinity for  $\omega_1 \rightarrow 0$  and for  $\omega_2 \rightarrow 0$ . This increase in  $\sigma_0$  is counteracted by an increase of  $K_1$  or  $K_2$  with different signs of  $\sigma_0$  and  $K_k$ . Finite stresses are only possible if for  $\omega = 0$  the ratio  $K/\sigma_0$  is finite. This is shown in Fig. 6 where  $K_1/\sigma_0$  is plotted versus  $\omega_1$  and  $K_2/\sigma_0$  versus  $\omega_2$ . For  $\omega_1 = 0$  there is  $K_1/\sigma_0 = -1$  and for  $\omega_2 = 0$  there is  $K_2/\sigma_0 = -1$ .

For the already mentioned examples the stress distribution is considered in detail.  $K_1$  and  $K_2$ , the exponents  $\omega_1$  and  $\omega_2$ , and the stress  $\sigma_0$  are given in Table 1. Figures 7 and 8 show the stress distributions near the free edge of the interface for  $\tau_{r\theta}$  along  $\theta = 0$ ,  $\sigma_r$  along  $\theta = \theta_1$  and  $\theta = \theta_2$  and  $\sigma_r, \sigma_\theta, \tau_{r\theta}$  along  $\theta = -22.5^\circ$ . The calculated stresses by means of FEM and analytical form are given. The stresses from the analytical form are the sum of

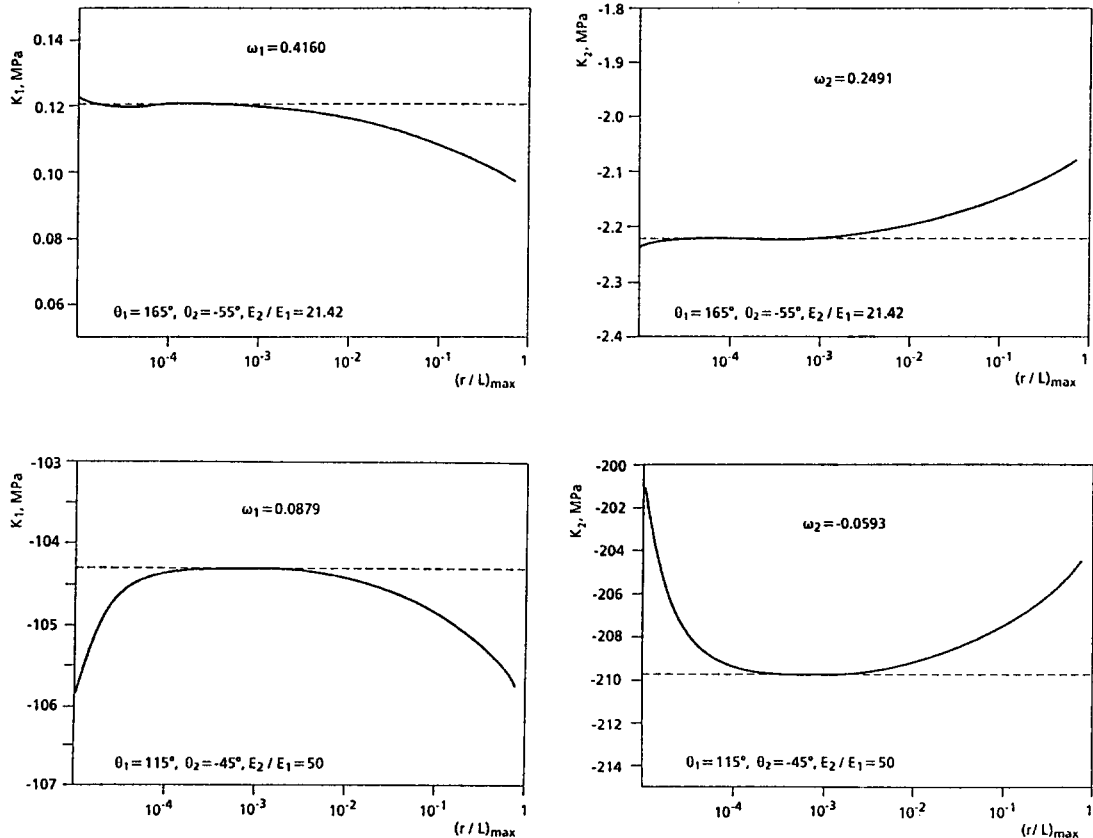


Fig. 4. Evaluated stress intensity factor versus upper bound of the range of  $r/L$  (thermal loading).

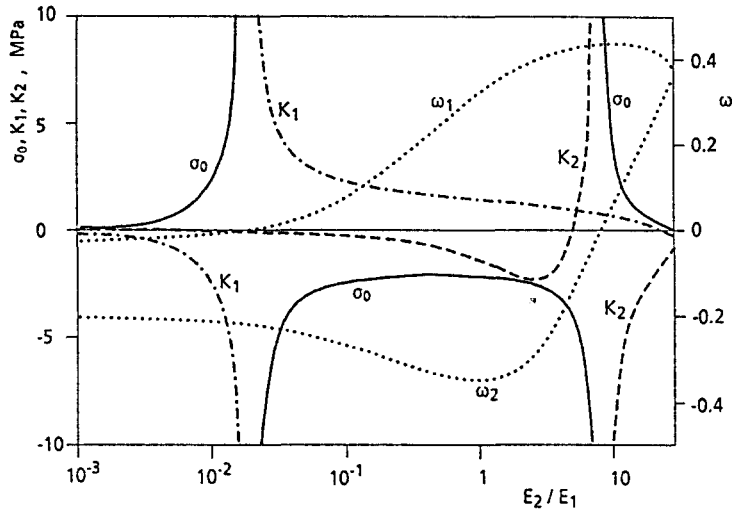


Fig. 5.  $\omega_1, \omega_2, K_1, K_2, \sigma_0$  versus  $E_1/E_2$  (combination A, thermal loading).

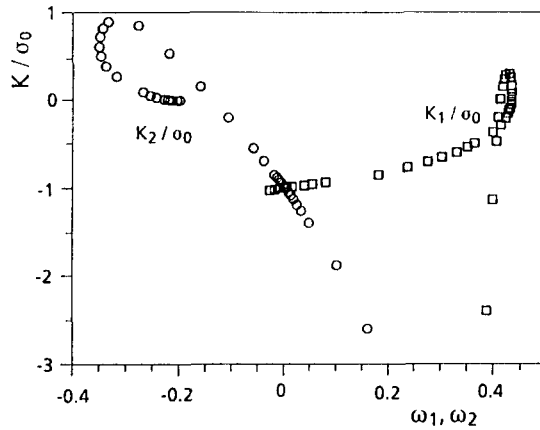


Fig. 6.  $K_1/\sigma_0$  versus  $\omega_1$  and  $K_2/\sigma_0$  versus  $\omega_2$  (combination A, thermal loading).

Table 1. Parameters for two examples

$\theta_1$	$\theta_2$	$E_2/E_1$	$\omega_1$	$\omega_2$	$K_1$ [MPa]	$K_2$ [MPa]	$\sigma_0$ [MPa]
$165^\circ$	$-55^\circ$	21.42	0.4160	0.2491	0.121	-2.223	0.499
$115^\circ$	$-45^\circ$	50.00	0.0879	-0.0593	-104.2	-210.3	306.1

three terms

$$\sigma_{ij} = \sigma_{ij0} + \sigma_{ij1} + \sigma_{ij2} = \sigma_{ij0} + \frac{K_1}{(r/L)^{\omega_1}} f_{ij1} + \frac{K_2}{(r/L)^{\omega_2}} f_{ij2}. \quad (9)$$

The figures show separately the terms  $\sigma_{ij0}, \sigma_{ij1}$  and  $\sigma_{ij2}$ .

For the example shown in Fig. 7 the two stress exponents are positive ( $\omega_1 = 0.4160, \omega_2 = 0.2491$ ). The stress intensity factors have different signs ( $K_1 = 0.121$  MPa,  $K_2 = -2.223$  MPa). The contribution of  $\sigma_{ij0}$  is small compared to that of  $\sigma_{ij1}$  and  $\sigma_{ij2}$ . It can

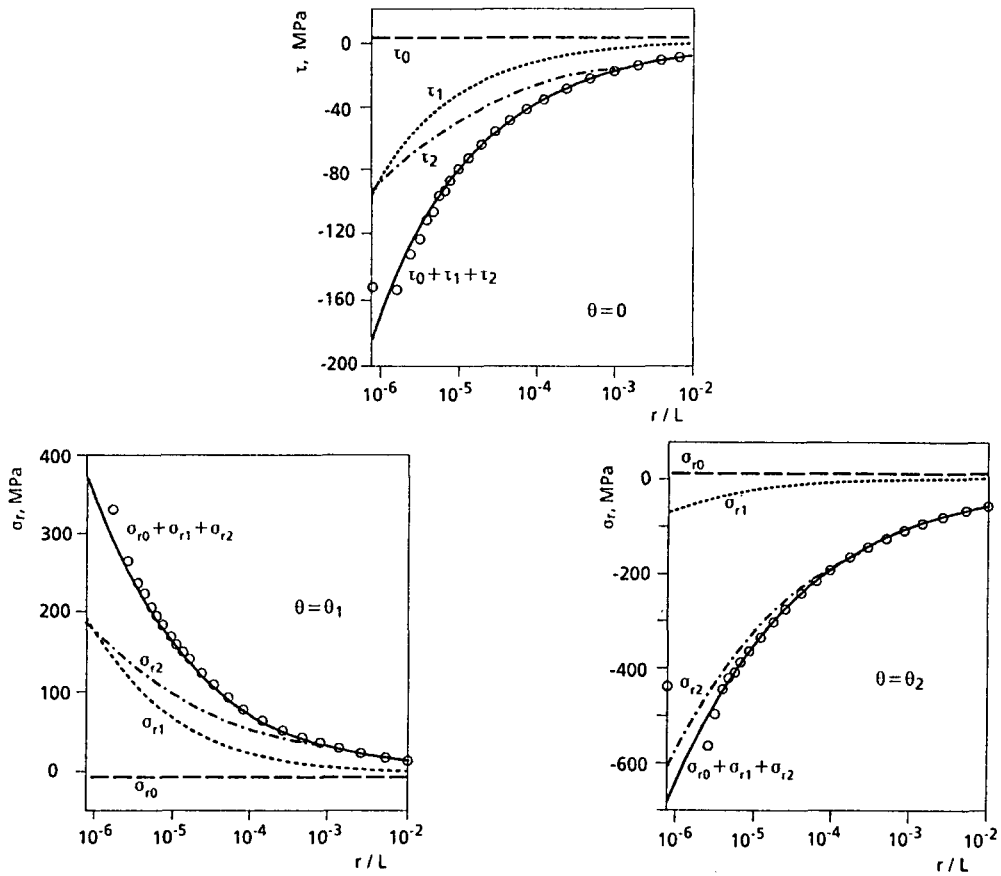


Fig. 7. Stresses versus  $r/L$  ( $\theta_1 = 165^\circ$ ,  $\theta_2 = -55^\circ$ , thermal loading,  $E_2/E_1 = 21.42$ , circles: FEM).

be seen that the term  $\sigma_{ij2}$  with the smaller stress exponent contributes significantly to the stress distribution. For  $\sigma_r$  at  $\theta = \theta_2$  the  $\sigma_{r2}$  term dominates.

For the example shown in Fig. 8 the stress exponents are small and have different signs ( $\omega_1 = 0.0879$ ,  $\omega_2 = -0.0593$ ). The stress intensity factors are negative and larger compared to the example in Fig. 7 ( $K_1 = -104.2$ ,  $K_2 = -210.3$ ). The contribution of  $\sigma_0$  is important in this example. The nonsingular term  $\sigma_{ij2}$  ( $\omega_2$  negative) contributes significantly to the stress distribution even at very small values of  $r/L$ .

Figure 9 shows results for combination A with mechanical loading. A constant load distribution is applied at the upper and lower surfaces, leading to a nominal stress  $\sigma_n$  at the interface. The regular stress term  $\sigma_{ij0}$  is zero. In contrast to the thermal loading the stress intensity factors  $K_1$  and  $K_2$  are finite for  $\omega_1 = 0$  and  $\omega_2 = 0$ . For  $E_2/E_1 = 21.42$ , the stress terms  $\tau_1$  and  $\tau_2$  are shown in Fig. 10. In contrast to the thermal loadings condition the contribution of the term  $\tau_2$  is small.

The Figs. 7, 8, and 10 show also a comparison of the results from the analytical relation and from FEM. The stress intensity factors  $K_1$  and  $K_2$  for the analytical relation have been determined – as already mentioned – from  $\sigma_\theta$  at  $\theta = 0$ . The comparison shows that for all stress components and different  $\theta$  the agreement between analytical results and FE-calculations is excellent. Only very close to the free edge deviations occur due to the inaccuracies in the FE-method [7]. Thus it is proved that the method is accurate.

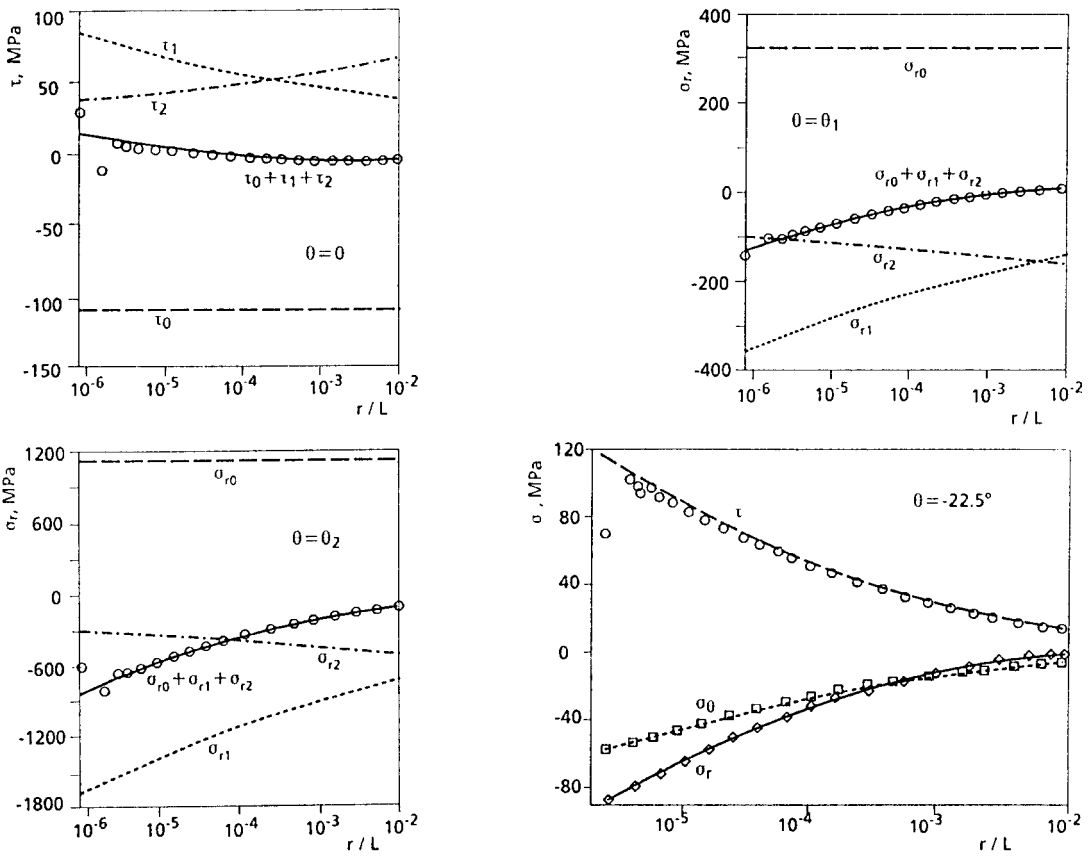


Fig. 8. Stress versus  $r/L$  ( $\theta_1 = 115^\circ$ ,  $\theta_2 = -45^\circ$ , thermal loading,  $E_2/E_1 = 50$ , circles: FEM).

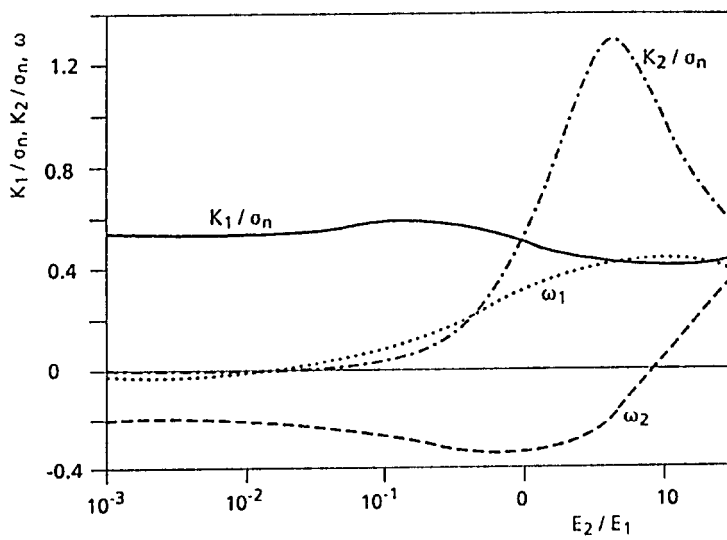


Fig. 9.  $\omega_1$ ,  $\omega_2$ ,  $K_1/\sigma_n$  and  $K_2/\sigma_n$  versus  $E_2/E_1$  (combination A, mechanical loading).



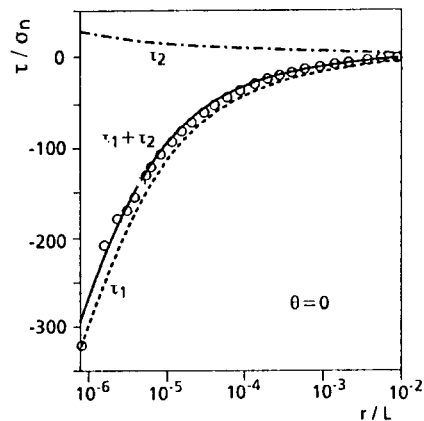


Fig. 10. Stress versus  $r/L$  ( $\theta_1 = 165^\circ$ ,  $\theta_2 = -55^\circ$ , mechanical loading,  $E_2/E_1 = 21.42$ , circles: FEM).

#### 4. Conclusions

1. A method based on finite element results was given, by which two or more stress intensity factors can be determined at the same time. There is a good agreement between the calculated stresses near the free edge of the interface of the bonded dissimilar materials from the analytical form with the determined stress intensity factors and those from FEM.
2. The stress distribution also very close to the free edge can be considerably influenced by the second term with  $\omega_2 < \omega_1$ . Even for  $\omega_2 < 0$ , i.e. no singularity, the second term may contribute significantly to the stresses. Also the term  $\sigma_{ij0}$ , which is independent of the distance from the free edge, can be very important for cooling stresses.
3. For a given geometry  $K_1$ ,  $K_2$  and  $\sigma_0$  approach infinity for specific material combinations. The corresponding stress exponent  $\omega_1$  and  $\omega_2$  are zero and the ratios  $K_1/\sigma_0$  and  $K_2/\sigma_0$ , respectively are  $-1$ . Thus the stresses are finite because the  $\sigma_0$ -term is balanced by the  $K_1$ - or  $K_2$ -term.
4. With the described procedure it is possible to select material combinations for a given geometry or a geometry (angles  $\theta_1$  and  $\theta_2$ ) for given material combinations with minimized stresses.

#### Acknowledgement

The financial support of the Deutsche Forschungsgemeinschaft is gratefully acknowledged.

#### References

1. D.B. Bogy, *Transactions ASME, Journal of Applied Mechanics* 38 (1971) 377–386.
2. V.L. Hein and F. Erdogan, *International Journal of Fracture Mechanics* 7(1971) 317–330.
3. D. Munz, T. Fett and Y.Y. Yang, *Engineering Fracture Mechanics* 44 (1993) 185–194.
4. Z. Knésl, A. Sramek, J. Kadourek and F. Kroupa, *Acta Techn. CSAV* 36 (1991) 574–593.
5. P.S. Theocaris, *The Mesophase Concept in Composites*, Springer, Berlin (1987).
6. Y.Y. Yang, dissertation, University of Karlsruhe, Germany, 1992.
7. J.D. Whitcomb, I.S. Raju and J.G. Goree, *Computer & Structures* 15 (1982) 23–37.